Changes in Protonation Associated with Substrate Binding and Cob(I)alamin Formation in Cobalamin-Dependent Methionine Synthase†

Joseph T. Jarrett,‡,§ Clara Y. Choi,|| and Rowena G. Matthews*,‡,||

Biophysics Research Division and Department of Biological Chemistry, University of Michigan, Ann Arbor, Michigan 48109-1055

Received August 11, 1997; Revised Manuscript Received October 13, 1997⊗

ABSTRACT: Methionine synthase catalyzes the transfer of a methyl group from methylcobalamin enzyme to homocysteine, generating methionine and cob(I)alamin enzyme, and then from methyltetrahydrofolate to cob(I)alamin enzyme, generating tetrahydrofolate and regenerating the methylcobalamin enzyme. The reactions catalyzed by methionine synthase require deprotonation of the substrate, homocysteine, and protonation of the product tetrahydrofolate, with no net change in proton stoichiometry for a complete turnover cycle. In addition, formation of the intermediate cob(I)alamin enzyme requires a change in the cobalt ligand geometry from 6-coordinate to 4-coordinate, and this rearrangement may require the transient protonation of protein residues to stabilize the cob(I)alamin enzyme. In the *E. coli* enzyme, the lower face of the methylcobalamin cofactor is coordinated by histidine 759, which is hydrogen bonded to aspartate 757 and then to serine 810, forming a "ligand triad". It has previously been shown that reduction of cob(II)alamin enzyme to cob(I)alamin is associated with the uptake of a proton from solution, and it has been postulated that this proton resides within the His759-Asp757 pair. Cob(I)alamin can also be generated by demethylation of methylcobalamin enzyme by homocysteine; it was not known whether this mode of cob(I)alamin formation was associated with proton uptake. In this paper, we use equilibrium titrations and kinetic analyses in the presence of the pH indicator dye phenol red, along with studies of the pH dependence of oxidation/reduction equilibria, to identify and characterize mechanistic steps associated with proton uptake and release in both the turnover and reactivation of the enzyme. We confirm that cob(I)alamin formation by reduction of cob(II)alamin enzyme is associated with proton uptake and show that mutation of Asp757 to Glu abolishes the pH dependence of this reduction. Demethylation of methylcobalamin enzyme also leads to cob(I)alamin formation and is also shown to be associated with proton uptake. By observing pre-steady-state reactions with homocysteine and methyltetrahydrofolate in the presence of phenol red, we show that this proton uptake occurs at a rate that is equal to the rate of formation of the cob(I)alamin enzyme. In addition, we show that binding of homocysteine to the enzyme results in the rapid release of a proton, presumably the homocysteine thiol proton. In contrast, binding methyltetrahydrofolate to the enzyme does not result in proton uptake, suggesting that the proton destined for the product tetrahydrofolate is already present on the free methylcobalamin enzyme.

Methionine synthase catalyzes the transfer of a methyl group from CH_3-H_4folate[1] to homocysteine, generating methionine and H_4folate. The cobalamin-dependent methionine synthase (MetH) from *Escherichia coli* catalyzes this reaction in two steps: the enzyme-bound methylcobalamin prosthetic group is first demethylated by homocysteine, generating methionine and the nucleophilic cob(I)alamin intermediate. This intermediate is remethylated by CH_3-H_4folate, producing H_4folate and regenerating the resting methylcobalamin enzyme (Figure 1). Occasional oxidation of the cob(I)alamin intermediate leads to an inactive cob(II)alamin enzyme; this species is returned to the catalytic cycle by a reductive methylation that uses flavodoxin and AdoMet as electron and methyl donors, respectively.

The reactions catalyzed by methionine synthase require changes in the protonation state of the substrates upon conversion to products, as well as potential transient changes in the protonation state of the enzyme during turnover and reactivation. Formation of methionine requires deprotonation of the homocysteine thiol proton [pK_a = 10.0 (*1*)] followed by nucleophilic attack of the thiolate anion on the methylcobalamin cofactor. Remethylation of the cob(I)alamin cofactor by CH_3-H_4folate requires protonation of N5 of the product H_4folate [pK_a = 4.8 (*2*)]. This protonation event may occur prior to or concurrent with methyl transfer to the cofactor and has been proposed as a possible mode of activation of CH_3-H_4folate towards nucleophilic attack (*3*, *4*). In addition, formation of the intermediate cob(I)alamin enzyme requires a change in the cobalt ligand geometry from 6-coordinate to 4-coordinate; in model systems, this is

† This research has been supported by NIH Research Grant R37 GM24908. J.T.J. was supported in part by NIH postdoctoral fellowship Grant F32 GM17455. C.Y.C is a trainee in the Medical Scientist Training Program at the University of Michigan funded by Grant T32 GM07863.

* Correspondence should be directed to this author at Biophysics Research Division, University of Michigan, 4024 Chemistry Building, 930 N. University Avenue, Ann Arbor, MI 48109-1055.

‡ Biophysics Research Division.

§ Present address: Department of Biochemistry and Biophysics, University of Pennsylvania School of Medicine, Philadelphia, PA 19104.

|| Department of Biological Chemistry.

⊗ Abstract published in *Advance ACS Abstracts,* December 1, 1997.

[1] Abbreviations: AdoMet, *S*-adenosyl-L-methionine; DTNB, 5,5′-dithiobis(2-nitrobenzoic acid); EDTA, ethylenediaminetetraacetic acid; Hcy, L-homocysteine; CH_3-H_4folate, 5-methyltetrahydrofolate; SHE, standard hydrogen electrode; H_4folate, 5,6,7,8-tetrahydrofolate; TEMPO, 2,2,6,6-tetramethyl-1-piperidinyloxy.

S0006-2960(97)01987-9 CCC: $14.00

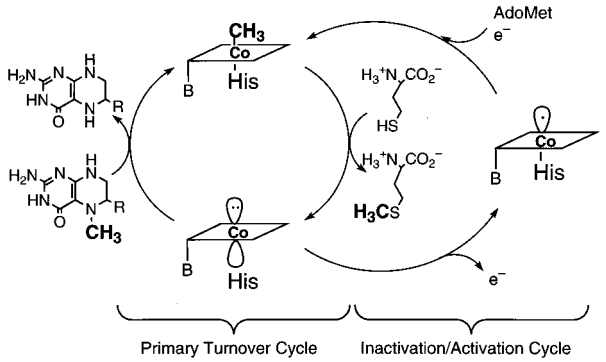

FIGURE 1: Schematic view of the reactions catalyzed by methionine synthase. In the primary turnover cycle, homocysteine and CH_3-H_4folate bind to the enzyme in a ternary complex prior to methyl transfer from methylcobalamin to homocysteine. Methyl transfer from CH_3-H_4folate to cob(I)alamin completes the reaction cycle prior to product release. Inactive enzyme is formed by one electron oxidation of the cob(I)alamin intermediate. The cob(II)alamin enzyme is returned to the primary turnover cycle by a electron transfer from reduced flavodoxin and methyl transfer from AdoMet.

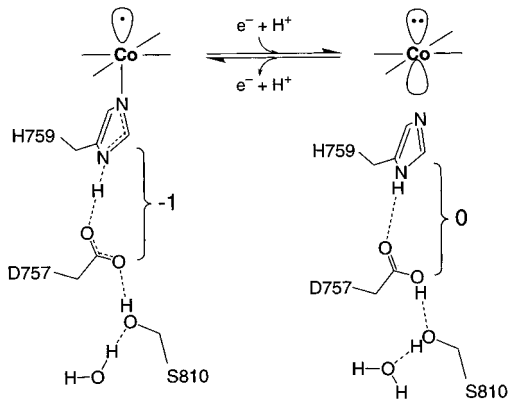

FIGURE 2: Proposed protonation of the ligand triad during reduction of cob(II)alamin enzyme. The midpoint potential for this reduction is pH dependent over the pH range 6.6−7.8, suggesting that reduction and/or ligand dissociation is accompanied by protonation of the enzyme (*19*). The structure of the B_{12}-binding region shows a hydrogen-bonded ligand triad His759-Asp757-Ser810, which we propose is protonated during cob(II)alamin reduction. The brackets indicate a net charge of −1 distributed over His759 and Asp757 in the oxidized enzyme; this charge is neutralized by protonation in the reduced enzyme.

facilitated by dissociation and protonation of the dimethylbenzimidazole ligand to the cobalt (*5*). In a similar manner, protonation of protein residues ligated to the cofactor may facilitate formation of the 4-coordinate cob(I)alamin enzyme.

A 3.0 Å resolution X-ray structure of the cobalamin-binding region of methionine synthase has been obtained (*6*), and the resolution has recently been extended to 2.4 Å (C. L. Drennan, and M. L. Ludwig, unpublished data). This structure reveals that the methylcobalamin cofactor undergoes a major conformational change on binding to methionine synthase. The dimethylbenzimidazole ligand to cobalt in the free cofactor dissociates from the cobalt on binding and is replaced by a histidine residue from the protein. As diagrammed in Figure 2, His759 is hydrogen bonded to Asp757, which in turn is hydrogen bonded to Ser810. His759 and Asp757 are shielded from solvent by protein residues and the cobalamin cofactor, and only Ser810 has access to solvent. These three residues are conserved in the six sequences for methionine synthase currently in the database, from *E. coli* (*7*, *8*, *9*), *Haemophilus influenzae* (*10*), *Mycobacterium leprae* (*11*), *Synechocystis* sp. (*12*), *Caenorhabditis elegans* (*13*), and *Homo sapiens* (*14*, *15*, *16*). The His-Asp-Ser triad has an important role in catalysis: mutation of His759 to Gly completely abolishes activity, while mutation of Asp757 to Glu or Asn decreases activity ∼20-fold (*17*, *18*). The triad forms a hydrogen-bonded network that could allow control of the protonation state of His759, which may be important in stabilizing 4-coordinate cob(II)alamin and cob(I)alamin species and/or in facilitating their interconversion.

Earlier studies had determined that reduction of enzyme-bound cob(II)alamin to cob(I)alamin was associated with proton uptake (*19*). In these studies, the midpoint potential of the cob(II)alamin/cob(I)alamin couple was shown to exhibit a −59 mV slope over the pH range from 6.6 to 7.4, consistent with the uptake of one proton on reduction of the cobalamin cofactor. An obvious candidate for protonation was the His759-Asp757 pair. Since cob(II)alamin is 5-coordinate both on the wild-type enzyme(*20*) and free in solution (*21*), while cob(I)alamin is preferentially 4-coordinate (*5*), it has been proposed that the His759-Asp757-Ser810 ligand triad shown in Figure 2 accepts a proton from solvent and dissociates from the cobalt on reduction of cob(II)alamin to cob(I)alamin (*6*). We have somewhat arbitrarily depicted the His759-Asp757 pair as having a net charge of −1 in Figure 2, and protonation would thus result in formation of a neutral His-Asp pair. By analogy to the conversion of cob(II)alamin to cob(I)alamin, conversion of 6-coordinate methylcobalamin to 4-coordinate cob(I)alamin could also be accompanied by proton uptake (*6*). However, it remained to be established whether this proton uptake occurs on a time scale which is relevant to catalysis and/or involves the ligand triad.

This paper examines the changes in protonation of the enzyme and substrates associated with catalysis and reactivation of the wild-type enzyme. We use the pH dependence of the cob(II)alamin/cob(I)alamin redox potential for wild-type enzyme and the Asp757Glu mutant enzyme to suggest that proton uptake occurs within the ligand triad upon reduction of cob(II)alamin enzyme. In order to distinguish proton uptake within the ligand triad from proton uptake or release due to substrate binding, we examine the binding of substrates to the inactive cob(II)alamin enzyme in the presence of the pH indicator dye phenol red. These experiments demonstrate the release of one proton upon binding homocysteine to the enzyme, but show no change in the protonation of the enzyme associated with CH_3-H_4-folate binding. We then use equilibrium titrations and enzyme-monitored stopped-flow spectroscopy in the presence of phenol red to provide evidence that kinetically competent proton uptake accompanies the formation of cob(I)alamin in the primary turnover cycle. We further confirm the protonation states of the cob(I)alamin and cob(II)alamin enzymes by oxidation of cob(I)alamin enzyme to cob(II)-alamin and by photolysis of methylcobalamin enzyme to cob-(II)alamin in the presence of phenol red.

MATERIALS AND METHODS

Materials. Construction of the Asp757Glu mutation of methionine synthase and the methods for expression and purification of wild-type and mutant enzymes have been described (*17*, *18*) The following compounds were obtained

from the indicated commercial sources and used without further purification: L-homocysteine thiolactone, *S*-adenosyl-L-methionine (iodide salt), dithiothreitol, and 5,5′-dithiobis-(2-nitrobenzoic acid) from Sigma; methyl viologen, phenol red, TEMPO, and protocatechuic acid from Aldrich; (6*R*,*S*)-CH_3-H_4folate (calcium salt) from Schirks Laboratories; and [^{14}C-*methyl*]-(6*R*,*S*)-CH_3-H_4folate (barium salt) from Amersham. Homocysteine thiolactone was hydrolyzed and neutralized prior to use in assays and titrations (*22*). 5-Deazaflavin-3-sulfonic acid was a gift from Professor Vincent Massey (University of Michigan), and protocatechuate dioxygenase was a gift from Professor David Ballou (University of Michigan). Phosphate buffer refers to potassium phosphate buffer at pH 7.2 unless otherwise specified.

Spectrophotometric Measurement of the Cob(II)alamin/Cob(I)alamin Midpoint Potential. The basic procedure for determination of the midpoint potentials as a function of pH was that described by Drummond and Matthews (*19*). A detailed method for determination of the midpoint potential is available as Supporting Information; a brief summary follows. A solution was prepared that contained cob(II)-alamin enzyme (20−40 μM), methyl viologen (100 μM), and 5-deazaflavin-3-sulfonate (5 μM) in a buffer of 100 mM potassium phosphate, 100 mM KCl, and 25 mM EDTA and was placed in an anaerobic quartz cuvette and equilibrated with argon. The sample was cooled to 0 °C and reduced by irradiation with a 600 W tungsten/halogen lamp. The contents of the cell undergo slow oxidation over 2−3 h, and spectra were recorded at 10 min intervals throughout the oxidation process. Extraction of the midpoint potential for each sample requires determination of the system potential and the relative concentrations of cob(II)alamin and cob(I)-alamin enzyme for each spectrum. Changes in the cobalamin spectra are approximately isosbestic at 600 nm for wild-type and Asp757Glu enzymes; changes at these wavelengths were used to determine the concentration of reduced methyl viologen cation radical using $\epsilon_{600} = 13\,600$ (*23*). The cell potential was determined from the concentration of reduced and oxidized methyl viologen using a midpoint potential of −446 mV vs SHE (*23*). The concentration of cob(II)alamin and cob(I)alamin enzyme was determined for each spectrum from the absorbance at 474 and 466 nm for wild-type and Asp757Glu enzymes,[2] respectively, after correcting for the smaller spectral changes at these wavelengths attributable to methyl viologen. At this point, a Nernst plot of cell potential vs log [cob(II)alamin/cob(I)alamin] allows estimation of the cobalamin midpoint potential for each sample. The standard error is approximately ±10 mV for each determination.

Determination of Proton Release in Equilibrium Titrations. Proton release accompanying the binding or reaction of homocysteine with wild-type enzyme, the oxidation of cob(I)alamin enzyme, and the photolysis of methylcobalamin enzyme was monitored in the presence of phenol red. These experiments were modeled after proton stoichiometry studies of lipoamide dehydrogenase (*24*) and D-amino acid oxidase (*25*). Details of the procedure for using phenol red in titrations and rapid kinetic experiments and for calculating stoichiometries are available as Supporting Information; a brief summary follows. For each titration, a solution was prepared that contained enzyme (20 μM) and phenol red (40 μM) in a buffer containing 50 μM potassium phosphate and 100 mM KCl at pH 7.8, placed in an anaerobic cuvette and equilibrated with argon. Titration of enzyme samples with 10 mM NaOH or HCl allowed determination of a stoichiometry conversion factor of $-0.0063\Delta A558/\mu M\ H^+$ released into solution. A sample of cob(II)alamin enzyme and phenol red (40 μM) was titrated with homocysteine (2 mM) and phenol red (40 μM), and spectra were recorded after each addition. After correcting for dilution, conversion of the spectral changes at 558 nm to the change in H^+ concentration allows construction of a binding curve for homocysteine. Alternatively, a sample of methylcobalamin enzyme and phenol red (40 μM) was titrated with homocysteine and phenol red, resulting in spectral changes associated with cob(I)alamin formation and H^+ release; deconvolution of these spectral changes is described in the Supporting Information. To examine proton release during cob(I)alamin oxidation, a sample of cob(I)alamin enzyme was produced by addition of 1 equiv homocysteine to methylcobalamin enzyme and phenol red (40 μM), and was then oxidized by titrating with potassium ferricyanide (2 mM). Finally, a sample of methylcobalamin enzyme was exposed to a 100 W tungsten lamp in the presence of TEMPO (400 μM) and phenol red (40 μM) to examine H^+ release during photolysis.

Enzyme-monitored stopped-flow experiments in the presence of phenol red were performed to examine the kinetic competence of proton uptake and release events. Methylcobalamin enzyme and phenol red (40 μM) were equilibrated with argon in one syringe, while homocysteine (200 μM), (6-*R*,*S*)-CH_3-H_4folate (800 μM) and phenol red (40 μM) were equilibrated with argon in the second syringe. Spectra of the samples were recorded prior to mixing and used to estimate an initial absorbance for the mixed sample prior to any reaction. After mixing, kinetic traces were obtained at 389, 480, and 558 nm, and the absorbance changes were deconvoluted as described in the Supporting Information.

Determination of CH_3-H_4Folate Binding by Equilibrium Dialysis. Radiolabeled [^{14}C-*methyl*]CH_3-H_4folate was prepared as described previously for our standard steady state assays (*26*), except that the specific activity was increased to ∼20 000 dpm/nmol. Both the enzyme and the CH_3-H_4-folate were prepared in a buffer containing 100 mM potassium phosphate, 8 mM sodium ascorbate, and 0.5 mM EDTA, pH 7.2. The enzyme (1.2 nmol in 60 μL) was placed in the inverted cap of a 0.5 mL microfuge tube, a small piece (∼2 × 2 cm) of presoaked, damp dialysis tubing (∼12 kD cutoff) was placed over the protein solution, and the inverted microfuge tube was pressed over the tubing and cap. A small hole was cut in the bottom of the microfuge tube and the CH_3-H_4folate solution (0.5−10 nmol in 200 μL) was added to the top of the dialysis membrane. The tubes were capped with parafilm and incubated in the dark at room temperature for 15 h. At this time, a portion of the upper solution containing only free substrate (50 μL) was transferred to a scintillation vial, and the remainder of the free substrate solution was removed by inverting the tube in a 1.5 mL microfuge tube and spinning at 500 rpm in a microcentrifuge. The enzyme plus bound substrate solution (50 μL) was removed by piercing the dialysis membrane with a syringe and was transferred to a separate scintillation vial. The initial substrate mix was a racemic mixture of (6*S*)- and (6*R*)-CH_3-

[2] Spectra of the wild-type and Asp757Glu enzyme in each of the oxidation states described in this paper are available as Supporting Information.

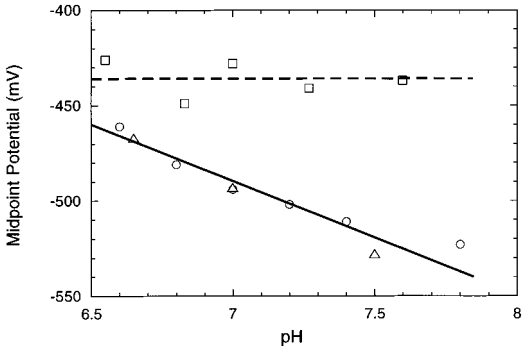

FIGURE 3: Midpoint potential for reduction of cob(II)alamin enzyme to cob(I)alamin enzyme measured as a function of pH for the wild-type enzyme (circles and triangles) and for the Asp757Glu mutant enzyme (squares). The solid line shows a theoretical slope of −59 mV expected for the uptake of one proton upon reduction of the wild-type enzyme. A linear least-squares fit gives an actual slope of −56 ± 6 mV. The dashed line indicates that no significant pH dependence was observed for the reduction of the Asp757Glu mutant enzyme. The data for the wild-type enzyme includes data (circles) from experiments described by Drummond and Matthews (*19*) that have been recalculated using the revised extinction coefficients cited in Materials and Methods.

H_4folate, but the bound substrate is assumed to be only the natural 6*S* isomer. The free (6*S*)-CH_3-H_4folate was calculated from the initial total CH_3-H_4folate by subtracting the calculated counts due to (6*R*)-CH_3-H_4folate. The concentrations of bound and free (6*S*)-CH_3-H_4folate are determined by eqs 1 and 2, where SA is the specific activity of [^{14}C-*methyl*]CH_3-H_4folate in counts per minute per nanomole.

$$[CH_3\text{-}H_4\text{folate}]_{bound} = [cpm_{enzyme\ soln} - cpm_{substrate\ soln}]SA^{-1}(0.05\ mL)^{-1} \quad (1)$$

$$[CH_3\text{-}H_4\text{folate}]_{free} = [cpm_{substrate\ soln} - (cpm_{total}/2)(50\ \mu L/260\ \mu L)]SA^{-1}(0.05\ mL)^{-1} \quad (2)$$

RESULTS

Cob(I)alamin Formation by Reduction of Cob(II)alamin Enzyme Is Accompanied by Proton Uptake within the Ligand Triad. The wild-type cob(II)alamin prosthetic group is primarily 5-coordinate with His759 ligated to the lower axial position on the cobalt. Reduction to the cob(I)alamin oxidation state requires reorganization of the cobalt ligand environment to a planar 4-coordinate geometry (*5*) with dissociation of the histidine ligand. This reorganization would be favored by protonation of His759 or the hydrogen-bonded Asp757 residue; the resulting change in charge should weaken the bond between His759 and the cobalt, favoring formation of the 4-coordinate cofactor (Figure 2). The uptake of one proton upon reduction of cob(II)alamin enzyme was confirmed in the present study (Figure 3), and the data in Drummond and Matthews (*19*) was recalculated using revised extinction coefficients for the enzyme (*18*), giving a midpoint potential at pH 7 of $E_{m7} = -490 \pm 9$ mV. The linear least-squares fit slope of −56 ± 6 mV compares well with the theoretical slope of −59 mV predicted for the uptake of a one proton upon reduction of cob(II)alamin enzyme to cob(I)alamin enzyme. If the proton is taken up within the His-Asp-Ser hydrogen-bonded network, then a mutation that disrupts this network should affect the pH dependence of the midpoint potential. The midpoint potential for the Asp757Glu mutant enzyme was measured over a range from pH 6.6 to 7.6 and shows no pH dependence, giving an average midpoint potential of −436 ± 8 mV (Figure 3). Since this mutation completely abolished the pH dependence of reduction, we propose that the proton taken up upon reduction of the wild-type cob(II)alamin enzyme resides within the His759-Asp757 pair, as depicted in Figure 2.

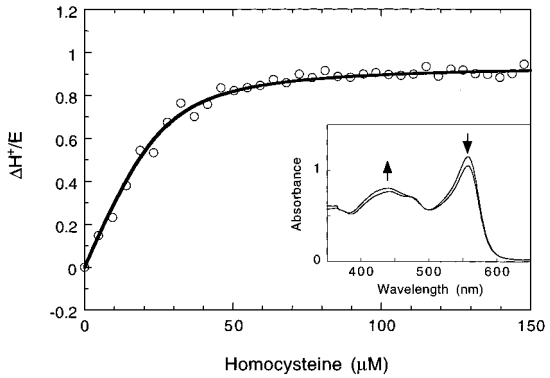

FIGURE 4: Titration of wild-type cob(II)alamin enzyme with homocysteine in the presence of phenol red in an anaerobic cuvette. The release of a proton upon formation of the enzyme:homocysteine complex results in a decrease in absorbance at 558 nm due to protonation of phenol red. See Materials and Methods for a description of the calculation of $\Delta H^+/E$ from these spectral changes. The initial pH was ∼7.8 and decreased less than 0.05 pH units during the course of the titration. The data shown are an average of five identical titrations and have been fit by a quadratic binding curve with the enzyme concentration fixed at 20 μM, giving an apparent K_d of 5 μM with the release of 0.9 equiv of protons. (Inset) Spectral change observed upon addition of 2 equiv homocysteine to cob(II)alamin enzyme (20 μM) and phenol red (40 μM) at pH 7.8.

Homocysteine Binding Is Accompanied by Release of One Proton. The methyl transfer reactions catalyzed by methionine synthase require the deprotonation of the substrate homocysteine and the protonation of the product tetrahydrofolate, resulting in no net change in proton concentration for a complete turnover cycle. We were able to characterize proton release due to homocysteine binding by titrating the inactive cob(II)alamin enzyme with homocysteine in the presence of the pH indicator dye, phenol red ($pK_a = 7.78$ determined experimentally), which shows a strong decrease in absorbance at 558 nm when the pH of the solution drops. Details of the titration procedure are described in the Materials and Methods and in accompanying Supporting Information.[2]

When homocysteine is added to cob(II)alamin enzyme in the presence of phenol red, there is a decrease in absorbance at 558 nm due to proton release from the enzyme:homocysteine complex and the subsequent protonation of phenol red (Figure 4, inset). This change in absorbance corresponds to the release of 0.9 ± 0.2 protons/mol methionine synthase with a K_d(observed) of 5 ± 3 μM at pH 7.8 (Figure 4). The presence of saturating CH_3-H_4folate had no effect on these results. The observed release of a proton suggests that the enzyme tightly binds the homocysteine thiolate anion, despite the relatively high microscopic pK_a of 10.0 measured for the homocysteine thiol (*1*). This observation was not unexpected, since neither methionine or homoserine is an effective competitive inhibitor for homocysteine ($K_i \geq 1$ mM). If it is assumed that the enzyme binds the homocysteine thiolate tightly, but that protonated homocysteine is bound to the enzyme with an affinity similar to that for

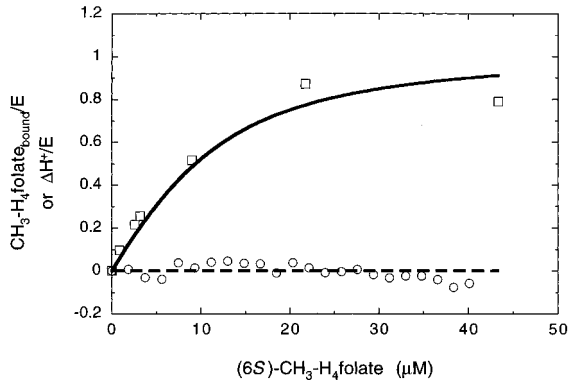

FIGURE 5: Binding of CH_3-H_4folate to wild-type cob(II)alamin enzyme. Equilibrium dialysis with radiolabeled CH_3-H_4folate was used to determine the affinity of cob(II)alamin enzyme for the substrate (squares). This data is fit to quadratic binding curve with the enzyme concentration fixed at 20 μM and gives a K_d of 5 μM. Titration of cob(II)alamin enzyme with CH_3-H_4folate in the presence of phenol red at pH 7.8 resulted in no changes in absorbance at 558 nm, indicating no uptake or release of protons upon formation of the enzyme:CH_3-H_4folate complex (circles).

methionine or homoserine, then eq 3 can be derived relating the true affinity for the thiolate anion to the observed affinity at the pH of the experiment. An estimated K_d for the thiolate

$$K_d(\text{observed}) = K_d(\text{thiolate})10^{(pK_a - pH)} \quad (3)$$

anion can be calculated to be ~30 nM. Several lines of evidence now suggest that release of a proton from the enzyme:homocysteine complex occurs when the thiolate anion becomes coordinated to a zinc atom whose binding site is localized to the N-terminal 353 amino acid residues of methionine synthase (*27*).

CH_3-H_4Folate Binding Is Not Accompanied by Proton Uptake or Release. Methyl transfer from CH_3-H_4folate to cob(I)alamin requires protonation of the product tetrahydrofolate. This proton could be taken up upon binding of CH_3-H_4folate to the enzyme or at a later stage of catalysis, such as just prior to or during methyl transfer from CH_3-H_4folate to cob(I)alamin. We titrated methylcobalamin enzyme with CH_3-H_4folate in the presence of phenol red. After correcting for dilution, we observed no net change in the spectrum of phenol red (Figure 5), suggesting that there was no proton uptake or release associated with formation of the enzyme: CH_3-H_4folate complex. In a separate experiment using radiolabeled CH_3-H_4folate, we measured the binding of CH_3-H_4folate to cob(II)alamin enzyme using equilibrium dialysis. This experiment confirmed that CH_3-H_4folate was binding to the enzyme over this concentration range with a K_d of 5 μM. Similar results were obtained using methylcobalamin enzyme. These results reproduce those of Taylor and Hanna, who showed that the affinity of CH_3-H_4folate for methionine synthase was pH independent and gave a K_d of 5 μM (*28*). These results demonstrate that CH_3-H_4folate binding is not associated with proton uptake and that the proton destined for N5 of H_4folate must be either already bound to the free enzyme or taken up at a later stage of the catalytic cycle.

Cob(I)alamin Formation during Turnover Is Accompanied by Proton Uptake. Cob(I)alamin enzyme is formed during the primary turnover cycle upon demethylation of methylcobalamin enzyme by homocysteine (Figure 1). Although the pH dependence of the equilibrium reduction of cob(II)alamin enzyme indicated that the His-Asp pair was protonated in the resulting cob(I)alamin enzyme, it was not clear whether the formation of cob(I)alamin during the primary turnover cycle would also be associated with proton uptake. To examine the proton stoichiometry upon conversion of methylcobalamin enzyme to cob(I)alamin enzyme directly, we took advantage of the ability of methionine synthase to catalyze the irreversible transfer of a methyl group from methylcobalamin enzyme to homocysteine in the absence of CH_3-H_4folate. The methylation of homocysteine to form methionine should result in the release of the thiol proton into solution. Thus, if the His759-Asp757 pair does not take up a proton upon conversion of methylcobalamin enzyme to cob(I)alamin enzyme, there should be stoichiometric proton release into solution; conversely, if the His759-Asp757 pair takes up a proton upon conversion of methylcobalamin enzyme to cob(I)alamin enzyme, there should be no net change in the pH of the solution. We observed that the initial formation of cob(I)alamin is not accompanied by a change in the absorbance of phenol red (Figure 6), suggesting that there is no net change in the pH of the solution. Thus, cob(I)alamin formation appears to be accompanied by protonation of the cob(I)alamin enzyme. After

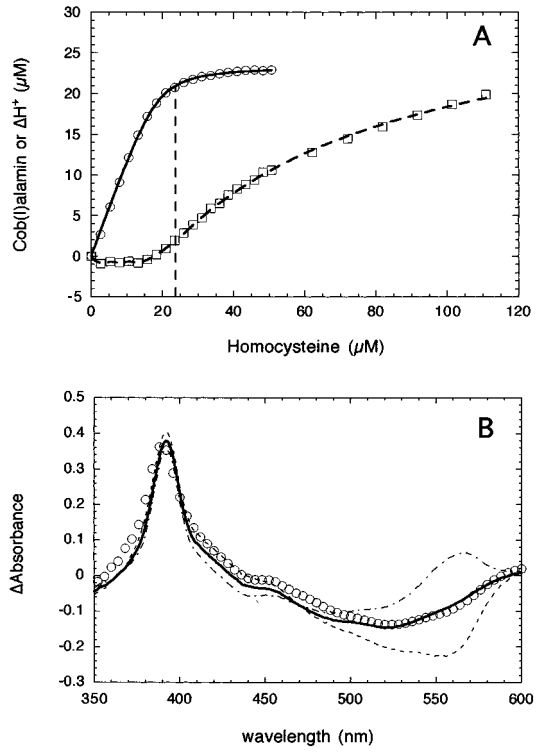

FIGURE 6: Proton uptake accompanying demethylation of wild-type methylcobalamin enzyme with homocysteine. (A) Titration of wild-type methylcobalamin enzyme with homocysteine in the presence of the phenol red at pH 7.8 in an anaerobic cuvette. Addition of 1 equiv of homocysteine (indicated by dashed vertical line) resulted in formation of 0.9 equiv of cob(I)alamin (circles and solid curve) and was accompanied by the release of ≤0.1 equiv of protons (squares and dashed curve). Since conversion of homocysteine to methionine results in release of one proton, cob(I)alamin formation must have been accompanied by uptake of ~0.8 proton by the enzyme. Further addition of homocysteine results in release of 1 equiv of protons due to the weak binding of homocysteine to the cob(I)alamin enzyme ($K_d \approx 25$ μM). (B) Difference spectrum generated by addition of 1 equiv homocysteine to the wild-type methylcobalamin enzyme (circles). The solid curve represents a fit assuming no net uptake or release of protons accompanying cob(I)alamin formation. For comparison, predicted difference spectra are shown for the uptake (− - − -) or release (- - - -) of a proton accompanying cob(I)alamin formation.

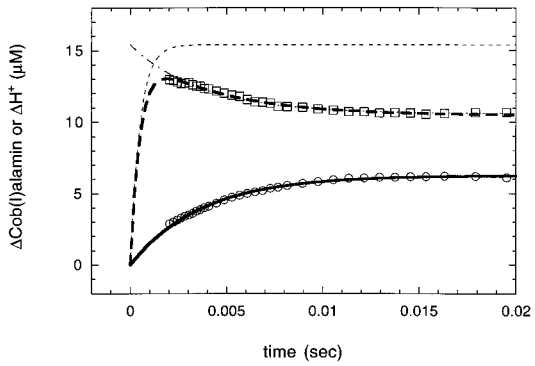

FIGURE 7: Reaction of wild-type methylcobalamin enzyme with homocysteine and CH_3-H_4folate in the presence of phenol red at pH 7.8 in an anaerobic stopped-flow spectrophotometer. Pre-steady-state formation of 6.2 μM cob(I)alamin, monitored at 390 nm, (circles and solid curve) is accompanied by uptake of 4.9 μM protons (squares and dashed curve). Differences between the predicted and observed initial absorbance indicate the release of 1 equiv of protons due to homocysteine binding within the dead time of the instrument and have been modeled using a rate constant of 2000 s^{-1} (− − − −). Uptake of a proton then accompanies cob(I)alamin formation and is fit to an apparent rate constant of 270 s^{-1} (− - − -).

conversion of ∼70% of the methylcobalamin enzyme to cob(I)alamin, a proton release event is observed to gradually compete with cob(I)alamin formation. This is likely due to the binding of a second equivalent of homocysteine to the cob(I)alamin enzyme, with a weak apparent K_d of ∼25 μM. To further confirm that cob(I)alamin formation was not accompanied by net proton uptake or release, we modeled the difference spectrum obtained upon addition of 1 equiv of homocysteine to the enzyme/phenol red solution (Figure 6B). Using separately obtained spectra of wild-type methylcobalamin and cob(I)alamin enzyme and of protonated and deprotonated phenol red, we were able to model the spectral data (open circles) to conversion of 22 μM methylcobalamin enzyme to cob(I)alamin (solid line), with no accompanying changes in the phenol red spectrum.

Although equilibrium titrations suggested that cob(I)alamin formation is accompanied by proton uptake, these titrations take several minutes to complete, and it is possible that this proton uptake does not occur within the ca. 20−30 ms lifetime of cob(I)alamin formed during steady state turnover. In order to establish the kinetic competence of proton release due to homocysteine binding and proton uptake which accompanies cob(I)alamin formation, we monitored turnover of the enzyme with homocysteine and CH_3-H_4folate in the presence of phenol red in an anaerobic stopped-flow spectrophotometer. Spectra of the enzyme/phenol red solution and of the substrate/phenol red solution were used to estimate an initial spectrum of the mixed sample prior to reaction. Comparison to the spectral data measured after rapidly mixing the samples in the stopped-flow instrument suggested that a proton had been released from the enzyme:substrate complex within the dead time of the instrument; we suggest that this proton release is due to rapid binding of homocysteine to the enzyme and release of the thiolate proton. We have modeled this proton release in Figure 7 with a rate constant of 2000 s^{-1}, although faster rates would be entirely consistent with the observed data.

After CH_3-H_4folate and homocysteine are bound to the enzyme, transfer of the methyl group from methylcobalamin to homocysteine results in formation of cob(I)alamin enzyme with a net pre-steady-state rate constant of 270 s^{-1}, as observed at 389 and 480 nm (Figure 7, circles). After correcting the spectral data at 558 nm for contributions due to changes in the spectrum of the cobalamin cofactor, we observe net changes in the spectrum of phenol red at 558 nm, which suggest the uptake of a proton by the enzyme:substrate complex at a rate of 250−300 s^{-1} (Figure 7, squares). By combining the predicted proton release due to homocysteine binding and proton uptake due to cob(I)alamin formation, we are able to model the observed transient changes in the proton stoichiometry, as shown by the heavy dashed curve in Figure 7. After 20 ms, a maximum of 6.2 μM cob(I)alamin is formed (40% of the total enzyme) and is accompanied by the uptake of 4.9 μM protons by the enzyme, giving a stoichiometry of $\Delta H^+/\Delta$Cob(I)alamin = 0.79.

Oxidation of Cob(I)alamin Formed during Primary Turnover to Cob(II)alamin Is Associated with Proton Release. Equilibrium titrations and rapid pre-steady-state reactions in the presence of phenol red suggest that conversion of methylcobalamin enzyme to cob(I)alamin is accompanied by proton uptake within the enzyme. However, these experiments are subject to spectral deconvolutions and corrections that could potentially skew the results. In order to confirm the protonation state of the cob(I)alamin cofactor formed during primary turnover, cob(I)alamin enzyme was formed by incubation of methylcobalamin enzyme with 1 equiv of homocysteine and was then oxidized to cob(II)alamin enzyme in the presence of phenol red by slow addition of potassium ferricyanide. Absorbance changes at 480 nm indicated that addition of 18 μM potassium ferricyanide led to oxidation of ∼15 μM cob(I)alamin enzyme (Figure 8A). This oxidation was accompanied by a decrease in absorbance at 558 nm that suggested the release of 0.73 equiv of protons into solution. The changes in the spectrum after addition of 1 equiv of potassium ferricyanide (Figure 8B, circles) were modeled using known spectra of wild-type cob(I)alamin and cob(II)alamin enzyme and of protonated and deprotonated phenol red. The best fit is obtained assuming stoichiometric proton release accompanies oxidation of cob(I)alamin to cob(II)alamin (solid curve).

Photolysis of Methylcobalamin Enzyme Is Not Associated with Changes in the Protonation State of the Enzyme. Formation of cob(I)alamin enzyme from either methylcobalamin or cob(II)alamin enzyme is associated with proton uptake, and we have hypothesized that this proton is taken up within the His759-Asp757 pair upon dissociation of His759 from the cobalt. This model predicts that the 6-coordinate methylcobalamin enzyme and the 5-coordinate cob(II)alamin enzyme should have the same net protonation state, since both enzyme forms have His759 coordinated to the cobalt. To confirm this, we photolyzed methylcobalamin enzyme in the presence of TEMPO and phenol red. TEMPO contains a nitroxide radical and is able to trap the methyl radical generated by photolysis, as shown in eqs 4 and 5, with no net change in protonation of either species. Changes

$$CH_3\text{-cobalamin} \xrightarrow{\text{light}} \text{cob(II)alamin} + CH_3^{\bullet} \quad (4)$$

$$CH_3^{\bullet} + \text{TEMPO-NO}^{\bullet} \rightarrow \text{TEMPO-NO-}CH_3 \quad (5)$$

in the spectrum of the wild-type enzyme photolyzed in the

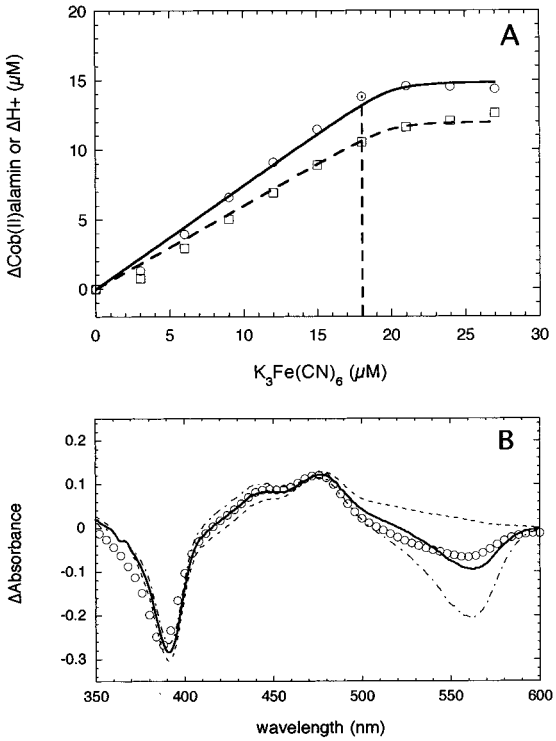

FIGURE 8: Oxidation of cob(I)alamin enzyme formed by demethylation of methylcobalamin enzyme in the presence of phenol red. Methylcobalamin enzyme is titrated with 1 equiv of homocysteine to generate cob(I)alamin enzyme. The cob(I)alamin enzyme is then oxidized to cob(II)alamin enzyme by slow addition of $K_3Fe(CN)_6$. (A) The addition of 18 μM $K_3Fe(CN)_6$ (dashed vertical line) results in formation of 15 μM cob(II)alamin enzyme (circles) and release of 11 μM H^+ (squares) by the enzyme, giving a stoichiometry of ΔH^+/cob(II)alamin = 0.73. (B) The difference spectrum generated by addition of 1 equiv $K_3Fe(CN)_6$ to the cob(I)alamin enzyme (circles) has been modeled assuming release of one proton accompanies oxidation of cob(I)alamin enzyme to cob(II)alamin (—). For comparison, predicted difference spectra are shown for release of two protons (— - — -) and for no net change in proton stoichiometry (- - - -).

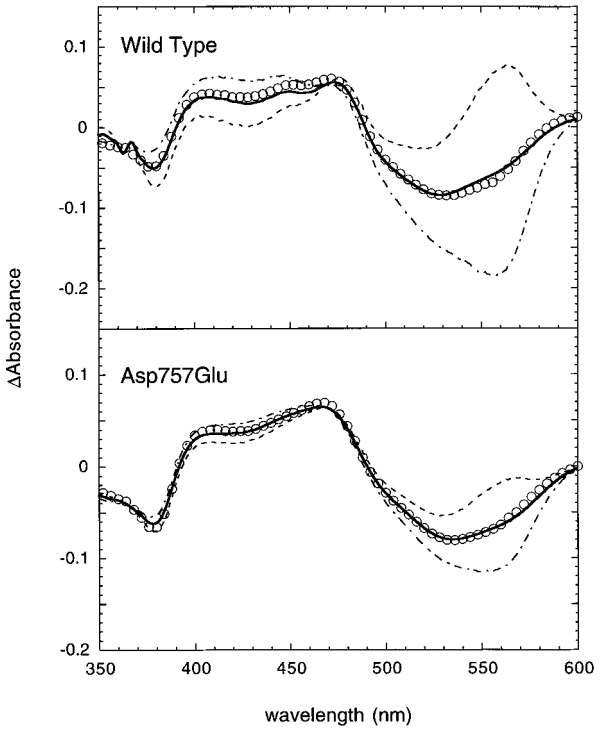

FIGURE 9: Conversion of wild-type (top panel) and Asp757Glu (bottom panel) methylcobalamin enzyme to cob(II)alamin enzyme by photolysis in the presence TEMPO and phenol red at pH 7.8. In each case, the observed difference spectrum (circles) is fit best assuming no change in the protonation state of the enzyme accompanies photolysis (—). For comparison, predicted difference spectra are shown in each case for the uptake (- - - -) or release (— - — -) of a proton accompanying cob(II)alamin formation.

presence of phenol red are shown in Figure 9 (upper panel). We are able to accurately model the spectral changes assuming no change in protonation of the enzyme, confirming that 6-coordinate methylcobalamin enzyme and 5-coordinate cob(II)alamin enzyme have similar net protonation states.

The Asp757Glu mutation was shown above to completely abolish the pH dependence of reduction of cob(II)alamin enzyme to cob(I)alamin (Figure 3). This could be due to the fact that the Asp757Glu enzyme is primarily 4-coordinate in the cob(II)alamin state (*18*) and, therefore, may already be protonated in the cob(II)alamin state. If this were the case, conversion of methylcobalamin enzyme to cob(II)alamin enzyme would be expected to be accompanied by uptake of a proton by the protein. Alternatively, the mutation of Asp757 to the larger Glu residue may have caused a structural change which abolished the ability to protonate and deprotonate His759 when this residue dissociates from or associates with the cobalamin cofactor (Figure 10). If this were the case, then all oxidation states of the Asp757Glu enzyme would have the same protonation state, and dissociation of His759 from the cobalt upon conversion of 6-coordinate methylcobalamin enzyme to 4-coordinate cob(II)alamin enzyme would be expected to be accompanied by no uptake or release of a proton by the protein (Figure 10). We photolyzed Asp757Glu methylcobalamin enzyme to 4-coordinate cob(II)alamin enzyme in the presence of TEMPO and phenol red, in a manner similar to that described above for the wild-type enzyme. Changes in the spectra accompanying photolysis (Figure 9, lower panel) are accurately modeled assuming no change in the protonation state of the Asp757Glu enzyme upon conversion from the 6-coordinate methylcobalamin enzyme to the 4-coordinate cob(II)alamin enzyme. These results suggest that all forms of the Asp757Glu enzyme have a similar net protonation state.

DISCUSSION

Methionine biosynthesis requires the transfer of a methyl group from CH_3-H_4folate to homocysteine; at neutral pH, the uncatalyzed reaction involves transfer of a methyl group from a tertiary amine to a protonated thiol. The enzyme presumably activates the nucleophile by deprotonation of homocysteine to the thiolate anion [pK_a = 10.0 (*1*)] and may activate the leaving group by protonation of CH_3-H_4folate to the quaternary amine [pK_a = 5.2 (*29*)]. We have observed that binding homocysteine to the enzyme results in the rapid release of 1 equiv of protons into solution, suggesting that the enzyme selectively binds the homocysteine thiolate anion. One possible strategy for selective binding of the homocysteine thiolate anion would be coordination of the sulfur to a metal. In the accompanying paper, Goulding and Matthews report that the overexpressed enzyme from *E. coli* contains one equiv of tightly bound zinc that is essential for binding homocysteine to the N-terminal substrate binding region (*27*).

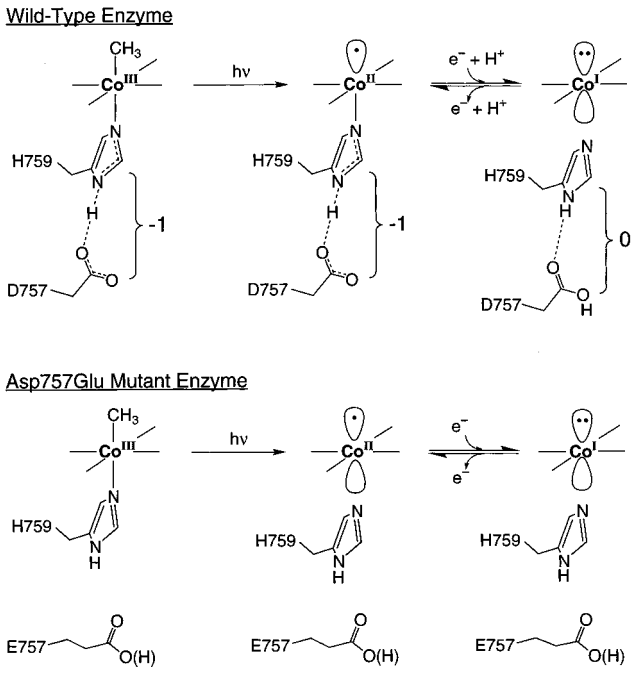

FIGURE 10: Scheme describing proposed changes in protonation of the His759-Asp757 pair accompanying dissociation of His759 during photolysis or methylcobalamin enzyme or reduction of cob(II)alamin enzyme. Photolysis of wild-type methylcobalamin enzyme to form 5-coordinate cob(II)alamin does not involve uptake or release of protons, while reduction of the wild-type cob(II)alamin enzyme to cob(I)alamin is accompanied by dissociation of His759 and proton uptake through the Asp757-Ser810 hydrogen bonded network. Photolysis of the Asp757Glu mutant enzyme is accompanied by dissociation of His759 and formation of 4-coordinate cob(II)alamin enzyme, but without proton uptake by the enzyme. We propose that the Asp757Glu mutation may have disrupted the hydrogen bond between His759 and the carboxylate and that the histidine residue is protonated in both the 6- and 4-coordinate enzyme. The charge state of Glu757 is not determined by these experiments, as indicated by (H).

The origin of the proton that is destined for N5 of H_4-folate remains unresolved by this study. Measurements of the binding of CH_3-H_4folate to the inactive cob(II)alamin and active methylcobalamin forms of the enzyme in the presence of phenol red suggest that a proton is not taken up upon formation of the enzyme:CH_3-H_4folate complex. Since homocysteine binding in the presence of CH_3-H_4folate is accompanied by proton release, and yet a complete turnover cycle involves no net change in proton concentration, the proton destined for N5 of H_4folate must be either already bound to the free methylcobalamin enzyme or taken up at a very late stage in each turnover cycle. The precise mechanism of this protonation event must await additional structural information.

Methyl transfer from the methylcobalamin cofactor to the bound homocysteine thiolate results in the formation of cob(I)alamin as a transient intermediate in steady state turnover. The cobalt of enzyme-bound methylcobalamin exhibits 6-coordinate (octahedral) ligation with the methyl group serving as the upper axial ligand, four equatorial nitrogen ligands provided by the corrin macrocycle, and Nϵ of His759 as the lower axial ligand (*6*). Cobalt in cob(I)alamin cofactor prefers planar 4-coordinate planar coordination geometry (*5*) provided by the four nitrogens of the corrin macrocycle. The enzyme must therefore dissociate and stabilize the lower axial histidine ligand upon conversion of methylcobalamin enzyme to cob(I)alamin. Reduction of 5-coordinate cob(II)alamin enzyme to 4-coordinate cob(I)alamin enzyme during the reductive methylation of oxidized enzyme also requires dissociation of the lower axial histidine ligand (Figure 1).

It has been reported that the reduction of cob(II)alamin enzyme to cob(I)alamin is coupled with the uptake of one proton by the enzyme (*19*), resulting in a midpoint potential for the cob(I)alamin/cob(II)alamin couple that is pH dependent over the range where the enzyme is stable (pH 6.5−8.0). Mutation of Asp757 to Glu abolishes this pH dependence, suggesting that the proton taken up by the wild-type enzyme resides within the His759-Asp757 pair. It has also been reported that binding the *in vivo* reductant, flavodoxin, to the 5-coordinate cob(II)alamin enzyme is coupled with a conformational change that leads to formation of the 4-coordinate cob(II)alamin enzyme and that the formation of the flavodoxin:methionine synthase complex is coupled with the uptake of one proton from solution (*30*). Again, the mutation Asp757Glu abolishes the pH dependence of flavodoxin association (*30*), suggesting that the proton taken up by the wild-type enzyme when flavodoxin binds resides within the His759-Asp757 pair. These reactions share common features: reduction of cob(II)alamin enzyme and binding flavodoxin to cob(II)alamin enzyme both require formation of a 4-coordinate cobalamin cofactor, and both reactions are apparently coupled with protonation of the His759-Asp757 pair.

Although the conversion of methylcobalamin cofactor to cob(I)alamin during the primary turnover cycle (Figure 1) was also be expected to be coupled to protonation of the His759-Asp757 pair, several factors made it experimentally difficult to establish proton uptake or release during this primary turnover cycle. The experiments cited above established proton uptake by measuring a shift in an equilibrium constant as a function of pH; however, the formation of the cob(I)alamin cofactor during turnover is coupled with the formation of a very stable carbon−sulfur bond in the product methionine and is therefore irreversible. We resorted to the direct detection of proton uptake or release using the pH indicator dye phenol red, observing spectral changes that suggest a proton is also taken up upon conversion of methylcobalamin enzyme to cob(I)alamin (Figures 6 and 7). This proton is taken up at a rate which is kinetically competent for involvement in the primary turnover cycle (Figure 7). Thus, the known forms of methionine synthase with 4-coordinate cobalamin cofactors, including cob(I)alamin generated by demethylation of methylcobalamin enzyme, cob(I)alamin generated by reduction of cob(II)alamin enzyme, and cob(II)alamin within the flavodoxin:methionine synthase complex, share the common feature of proton uptake within the His759-Asp757-Ser810 triad.

This proton uptake appears to be an important feature of cobalamin-dependent methionine synthase that has been preserved during evolution; the known sequences of methionine synthase, ranging from prokaryotes to humans, all feature the conserved His-Asp-Ser triad as part of the B_{12}-binding domain. The thermodynamic benefit of proton uptake for the formation of cob(I)alamin is apparent from model studies of the pH-dependent electrochemistry of cobalamins conducted by Saveant and co-workers (*5*, *31*). The reduction of free cob(II)alamin to cob(I)alamin requires a very low-potential electron [$E_{m7} = -610$ mV vs SHE (*31*)]. Part of this thermodynamic barrier is due to the energy

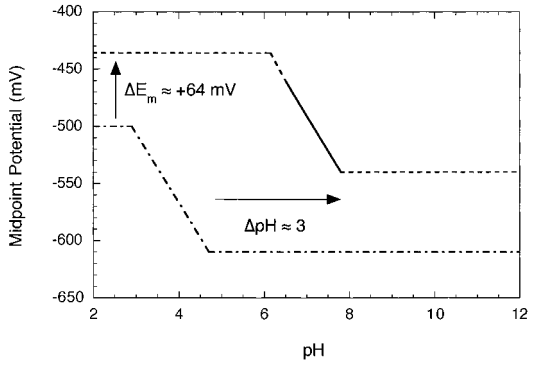

FIGURE 11: Binding the cobalamin cofactor to methionine synthase alters the pH profile of the midpoint potential for the cob(II)alamin/cob(I)alamin couple. At pH values above 4.9, the free cob(II)alamin cofactor (− - − -) requires a very low potential electron ($E_m = -610$ mV) for reduction to cob(I)alamin; however, below pH 2.9 this potential is raised due to protonation and dissociation of the dimethylbenzimidazole ligand (*31*). Between pH 2.9 and 4.7, the midpoint potential exhibits pH dependence. Binding cob(II)alamin to the enzyme (−) results in an increase in the overall midpoint potential by ∼64 mV, and replacement of dimethylbenzimidazole by the His759-Asp757-Ser810 triad results in a shift in the pH-dependent segment into the physiological range. The solid line represents the experimentally derived curve from Figure 3, while the dashed lines represent hypothetical extensions of this curve to low and high pH.

required to dissociate the lower axial dimethylbenzimidazole ligand; at pH values below 2.9, where the dimethylbenzimidazole ligand is already dissociated and protonated, reduction of cob(II)alamin to cob(I)alamin occurs with an E_m of −500 mV.

Binding cobalamin to methionine synthase is associated with two factors that act to raise the midpoint potential associated with reduction of enzyme-bound cob(II)alamin (Figure 11). First, reduction of free 5-coordinate cob(II)alamin to 4-coordinate cob(I)alamin is pH dependent over the narrow range from 2.9−4.7 (Figure 11); over the physiologic pH range the midpoint potential is invariant at −610 mV (*31*). Replacement of dimethylbenzimidazole with the His-Asp-Ser triad shifts the pH-dependent segment of the cob(II)alamin/cob(I)alamin couple into the physiological pH range (Figure 11). Second, binding cob(II)alamin to methionine synthase raises the overall redox potential for reduction of the 4-coordinate cob(II)alamin to cob(I)alamin by ∼64 mV [from −500 mV in the free cofactor (*31*) to −436 mV in the bound cofactor at pH <6 (Figure 11)]. We have estimated the pH-independent value of −436 mV for the wild-type enzyme from the value obtained for the Asp757Glu mutant enzyme. This conservative mutation, which is thought to perturb the hydrogen bond between His759 and Asp757, results in cob(II)alamin enzyme that is predominantly 4-coordinate throughout the physiological pH range (*18*). The combined effects of the shift in p*K* values for the bound and unbound lower axial ligand and the overall shift in the redox potential associated with binding cob(II)alamin to the enzyme raise the redox potential for the cob(II)alamin/cob(I)alamin couple from −610 mV for the free cofactor to −490 mV for the enzyme-bound cofactor at pH 7.

In addition to these thermodynamic benefits, protonation and dissociation of His759 may also lead to accelerated electron transfer rates during reductive methylation of cob(II)alamin enzyme. Binding flavodoxin to cob(II)alamin methionine synthase leads to dissociation of His759 from the cobalt, protonation of the His759-Asp757 pair, and formation of a 4-coordinate cob(II)alamin enzyme that has a similar coordination geometry to cob(I)alamin enzyme (*30*). Marcus theory predicts that preorganization of the metal center to more closely resemble the product will lead to faster electron transfer from reduced flavodoxin to the cobalt due to a decrease in the nuclear reorganization that must accompany the electron transfer step (*32*). Since the driving force for electron transfer from flavodoxin to cob(II)alamin is low [$\Delta E_{m7} = +40$ mV (*30*)], nuclear preorganization may be critical in accelerating the overall rate of electron transfer. Upon considering that a weak lower axial cobalt ligand appears to offer significant thermodynamic and kinetic advantages during reduction of cob(II)alamin enzyme, one might question whether nature should have evolved methionine synthase to more closely resemble the Asp757Glu mutant. Proton uptake observed upon conversion of methylcobalamin enzyme to cob(I)alamin appears to be relatively unimportant for the chemical events of methionine biosynthesis since the mutation Asp757Glu results in a relatively modest 3-fold decrease in the rate of methyl transfer from methylcobalamin to homocysteine (*18*). However, the Asp757Glu mutant is ∼20−30 fold impaired in overall steady state activity (*17*, *18*), primarily due to an uncharacterized kinetic step that we loosely attribute to conformational changes associated with product release. The strength of the coordination of His759 to the cobalt appears to be tuned to balance the thermodynamic and kinetic benefits of ligand dissociation accompanying cob(I)alamin formation during reductive methylation with the apparent importance of the His759-Asp757 pair in triggering product release during primary turnover.

ACKNOWLEDGMENT

We thank Professor David Ballou (University of Michigan) for the use of his stopped-flow apparatus.

SUPPORTING INFORMATION AVAILABLE

Detailed methods describing the determination of pH-dependent midpoint potentials for the cob(II)alamin/cob(I)alamin couple, the measurement of proton uptake and release using phenol red, and spectra of the methylcobalamin, cob(II)alamin, and cob(I)alamin forms of the wild-type and Asp757Glu enzymes (9 pages). Ordering information is given on any current masthead page.

REFERENCES

1. Benesch, R. E., and Benesch, R. (1955) *J. Am. Chem. Soc. 77*, 5877−5881.
2. Kallen, R. G., and Jencks, W. P. (1966) *J. Biol. Chem. 241*, 5845.
3. Matthews, R. G., and Drummond, J. T. (1990) *Chem. Rev. 90*, 1275−1290.
4. Matthews, R. G., Banerjee, R. V., and Ragsdale, S. W. (1990) *BioFactors 2*, 147−152.
5. Lexa, D., and Savéant, J.-M. (1983) *Acc. Chem. Res. 16*, 235−243.
6. Drennan, C. L., Huang, S., Drummond, J. T., Matthews, R. G., and Ludwig, M. L. (1994) *Science 266*, 1669−1674.
7. Banerjee, R. V., Johnston, N. L., Sobeski, J. K., Datta, P., and Matthews, R. G. (1989) *J. Biol. Chem. 264*, 13888−13895.
8. Drummond, J. T., Orgorzalek Loo, R. R., and Matthews, R. G. (1993) *Biochemistry 32*, 9282−9289.
9. Old, I. G., Margarita, D., Glass, R. E., and Saint Girons, I. (1990) *Gene 87*, 15−21.

10. Fleischmann, R. D., Adams, M. D., White, O., Clayton, R. A., Kirkness, E. F., Kerlavage, A. R., Bult, C. J., Tomb, J.-F., Dougherty, B. A., Merrick, J. M., McKenney, K., Sutton, G., FitzHugh, W., Fields, C., Gocayne, J. D., Scott, J., Shirley, R., Liu, L.-I., Glodek, A., Kelley, J. M., Weidman, J. F., Phillips, C. A., Spriggs, T., Hedblom, E., Cotton, M. D., Utterback, T. R., Hanna, M. C., Nguyen, D. T., Saudek, D. M., Brandon, R. C., Fine, L. D., Fritchman, J. L., Fuhrmann, J. L., Geoghagen, N. S. M., Gnehm, C. L., McDonald, L. A., Small, K. V., Fraser, C. M., Smith, H. O., and Venter, J. C. (1995) *Science 269*, 496−512.
11. Smith, D. R. (1994) GenBank accession no. U00017.
12. Kaneko, T., Tanaka, A., Sato, S., Kotani, H., Sazuka, T., Miyajima, N., Sugiura, M., and Tabata, S. (1995) GenBank accession no. D64002.
13. Swinburne, J. (1994) *Nature 368*, 32−38.
14. Leclerc, D., Campeau, E., Goyette, P., Adjalla, C. E., Christensen, B., Ross, M., Eydoux, P., Rosenblatt, D. S., Rozen, R., and Gravel, R. A. (1996) *Hum. Mol. Genet. 5*, 1867−1874.
15. Li, Y. N., Gulati, S., Baker, P. J., Brody, L. C., Banerjee, R., and Kruger, W. D. (1996) *Hum. Mol. Genet. 5*, 1851−1858.
16. Chen, L. H., Liu, M.-L., Hwang, H.-Y., Chen, L.-S., Korenberg, J., and Shane, B. (1997) *J. Biol. Chem. 272*, 3628−3634.
17. Amaratunga, M., Fluhr, K., Jarrett, J. T., Drennan, C. L., Ludwig, M. L., Matthews, R. G., and Scholten, J. D. (1996) *Biochemistry 35*, 2453−2463.
18. Jarrett, J. T., Amaratunga, M., Drennan, C. L., Scholten, J. D., Sands, R. H., Ludwig, M. L., and Matthews, R. G. (1996) *Biochemistry 35*, 2464−2475.
19. Drummond, J. T., and Matthews, R. G. (1994) *Biochemistry 33*, 3732−3741.
20. Banerjee, R. V., Harder, S. R., Ragsdale, S. W., and Matthews, R. G. (l990) *Biochemistry 29*, 1129−1135.
21. Kräutler, B., Keller, W., and Kratky, C. (1989) *J. Am. Chem. Soc. 111*, 8936−8938.
22. Drummond, J. T., Jarrett, J., Gonzalez, J. C., Huang, S., and Matthews, R. G. (1995) *Anal. Biochem. 228*, 323−329.
23. Mayhew, S. G. (1978) *Eur. J. Biochem. 85*, 535−547.
24. Matthews, R. G., Ballou, D. P., Thorpe, C., and Williams, C. H. J. (1977) *J. Biol. Chem. 252*, 3199−3207.
25. Fitzpatrick, P. F., and Massey, V. (1982) *J. Biol. Chem. 257*, 9958−9962.
26. Jarrett, J. T., Goulding, C., Fluhr, K., Huang, S., and Matthews, R. G. (1997) *Methods Enzymol. 281*, 196−213.
27. Goulding, C. W., and Matthews, R. G. (1997) *Biochemistry 36*, 15749−15757.
28. Taylor, R. T., and Hanna, M. L. (1972) *Arch. Biochem. Biophys. 151*, 401−413.
29. Zhao, S., Roberts, D. L., and Ragsdale, S. W. (1995) *Biochemistry 34*, 15075−15083.
30. Hoover, D. M., Jarrett, J. T., Sands, R. H., Dunham, W. R., Ludwig, M. L., and Matthews, R. G. (1997) *Biochemistry 36*, 127−138.
31. Lexa, D., and Savéant, J. M. (1976) *J. Am. Chem. Soc. 98*, 2652−2658.
32. Marcus, R. A., and Sutin, N. (1985) *Biochim. Biophys. Acta 811*, 265−322.

BI971987T